

Thermal Simulation and Experiment of Lunar Drill Bit in Vacuum

Jinsheng Cui, Xuyan Hou*, Deming Zhao, Yousong Hou, Qiquan Quan, Xiang Wu,
Zongquan Deng, Shengyuan Jiang, Dewei Tang

School of Mechatronics Engineering, Harbin Institute of Technology
No.92, Xidazhi Street, Nangang District, 150001, Harbin, China

*Corresponding author, e-mail: houxuyan@hit.edu.cn

Abstract

Drilling samples of lunar soil is an important and indispensable part of China's lunar exploration project. The drill bit temperature during the drilling process is one of the key concerns for scholars, especially for the hard lunar rock drilling in vacuum. In this article, the simulation analysis of drilling in atmosphere and vacuum is conducted. Moreover, a fiber grating temperature measuring system integrated with vacuum drilling system is established. Experiment on lunar rock stimulant in atmosphere and vacuum is taken out and compared.

Keywords: lunar drill bit, thermal characteristic, vacuum environment, FBG

Copyright © 2014 Institute of Advanced Engineering and Science. All rights reserved.

1. Introduction

According to China's lunar exploration project planning, the sampling device carried by the detector will collect lunar soil, depth about 2m from the lunar surface, with bedding information [1]. Considering the sampling depth, dry drilling process, temperature change of lunar soil [2], high vacuum lunar surface, poor thermal properties of lunar soil [3-5] and high solar radiation, the drill bit may reach very high temperature. The high temperature of drill bit will result in structural damage of drill bit. In addition, it also may take unknown effect to lunar soil, leading to poor sample quality.

In considering of the engineering requirement, basing on the drill bit structure and drilling procedure parameters, an experimental device in this paper is designed to simulating the excessive working condition, the vacuum environment and lunar rocks. Comparative simulation and temperature testing of drilling process are performed under atmospheric and vacuum condition, providing reference for design and optimization.

2. On-line Temperature Measuring System Based on Fiber Bragg Grating Sensor

Principle of fiber Bragg grating (FBG) sensor is shown in Figure 1.

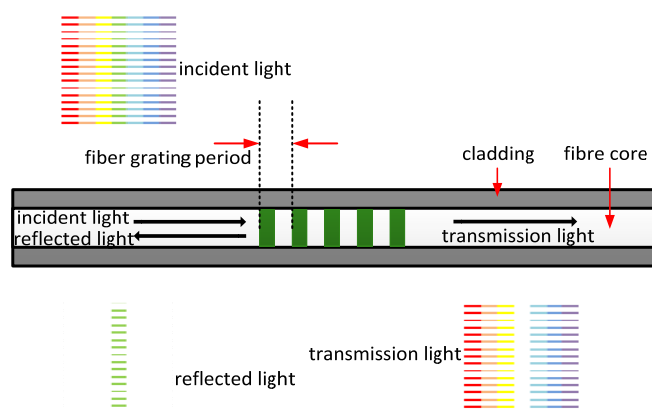


Figure 1. Schematic Beam Propagation within the Fiber

When a broadband beam transports to the fiber grating, since the band-stop role of filter grating, the Bragg wavelength of the light will return along the same route, and other wavelengths of light will pass through the grating. If the wavelength of the Bragg grating can be changed for some physical parameters, the change value can get by analyzing the reflection or transmission spectrum. The Bragg wavelength refers to the effective refractive index and the grating constant of the fiber core, which is as shown in formula (1).

$$\lambda_B = 2n_{\text{eff}}\Lambda \quad (1)$$

Where λ_B is Bragg wavelength; n_{eff} is Effective refractive index; Λ is Grating constant.

Differential form of formula (1) is as follows:

$$\frac{\Delta\lambda_B}{\lambda_B} = \frac{\Delta\Lambda}{\Lambda} + \frac{\Delta n_{\text{eff}}}{n_{\text{eff}}} \quad (2)$$

It can be seen from formula (2) that the physical quantities changing which can cause a change of the fiber Bragg grating refractive index or the grid spacing, will cause a change of the Bragg wavelength.

There are several facts can cause the Bragg wavelength drift due to the external temperature changes, such as the fiber expansion effect, the fiber thermal-optic effect and the photo-elastic effect. The photo-elastic effect is so weak that it can be ignored. Therefore, in a certain temperature range, when temperature influences FBG individually, the thermal expansion effect and the thermo-optic effect of the grating period and the effective refractive index change can be expressed as follows:

$$\frac{\Delta\Lambda}{\Lambda} = \alpha T \quad (3)$$

$$\frac{\Delta n_{\text{eff}}}{n_{\text{eff}}} = -\frac{1}{n_{\text{eff}}} \frac{dn_{\text{eff}}}{dV} \frac{dV}{dT} \Delta T \quad (4)$$

Where α is the thermal expansion coefficient of the fiber material; V is the normalized frequency of the fiber.

When the temperature changes, the drift of Bragg wavelength caused by the thermo-optical effect is denoted as:

$$\xi = -\frac{1}{n_{\text{eff}}} \frac{dn_{\text{eff}}}{dV} \frac{dV}{dT} \quad (5)$$

Where ξ is thermo-optic coefficient ($\xi = 6.67 \times 10^{-6}$).

The drift of FBG wavelength caused by temperature change can be denoted as:

$$\frac{\Delta\lambda_B}{\lambda_B} = (\alpha + \xi)\Delta T \quad (6)$$

FBG sensor has high precision, and its sensing results are rarely affected by the source energy or the optical path, adapting to the humid climate. And it also has capability of anti-electromagnetic interference, small size, easy to paste, and hardly impact on mechanical properties. Therefore FBG sensor is the best solution.

The fiber grating temperature measuring system is mainly composed of fiber Bragg grating sensors, optical fiber transmission line, optical signal demodulator, wireless transceiver device, PC and data processing software. FBG and the drill bit is shown in Figure 3. The measuring system is shown in Figure 2.

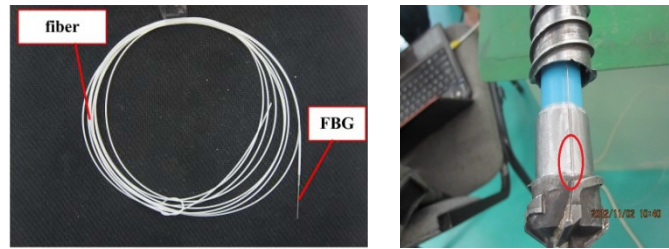


Figure 2. FBG and the Drill Bit

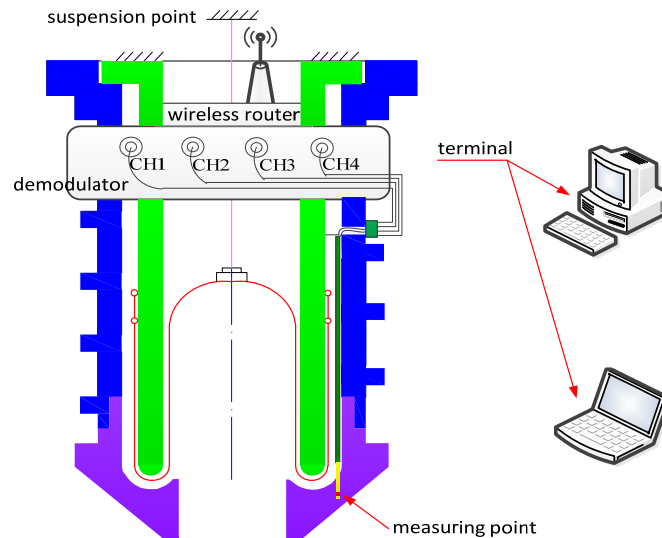


Figure 3. Schematic Diagram of FBG Test System

The transmission fiber of the FBG sensor is arranged along the drill pipe inside. And the sensor is installed in the drill near the cutting tool. The demodulation and a wireless module are installed on the host sampling drill rig, which can rotate with the drill rig. The PC receives data via a wireless module, then display and restore the data.

The experimental rig is shown (FBG sensor in drilling tool) in Figure 4.



Figure 4. Experimental Rig and Demodulator Installation

3. Simulation

Before the experiment, simulations comparison between drilling in atmosphere and vacuum are conducted. The main difference between the two conditions is convection. For

vacuum experiment, convection is ignored and radiation is considered in vacuum container, meanwhile, radiation is ignored and convection is considered out of vacuum container. For atmosphere experiment, convection is always considered, and radiation is the same as that in vacuum experiment. The heat transfer diagrams are shown in Figure 5.

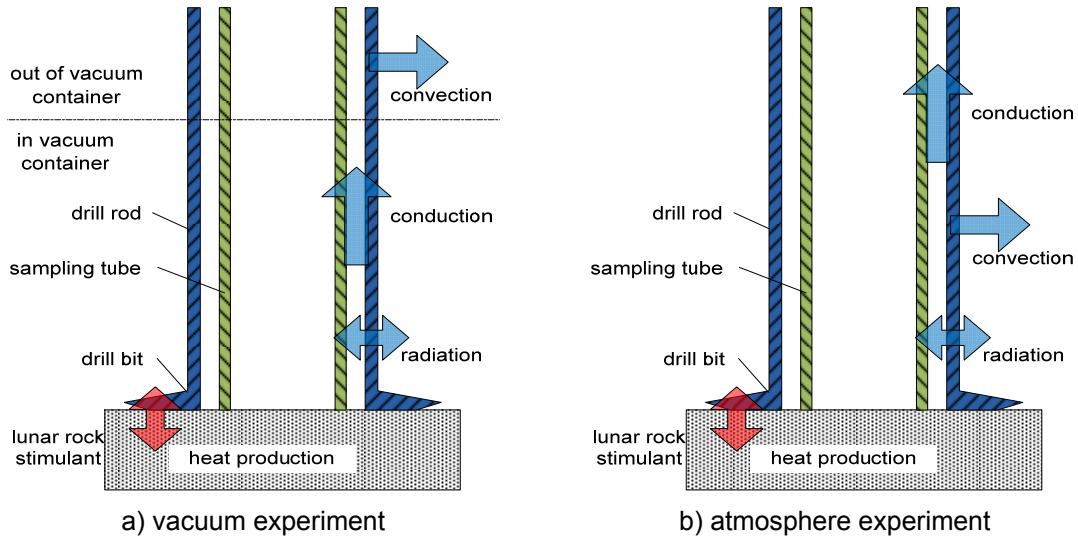


Figure 5. Heat Transfer Diagrams of Drilling Experiment

In order to simplify the analysis, change of cutting condition due to temperature rise is not considered in the simulation. Assume that heat is generated on the surface between cutting edge and rock. Part of the heat enters into the drill and the other enters into the rock. The heat generation for every cutting edge is given:

$$q_e(t) = \frac{1}{4}kP(t) = \frac{1}{4}kT(t)n \tag{7}$$

Where P(t) is power consumed on the motor, W; k is equivalent correction coefficient due to the factors of heat conversion, heat partition and so on, determined difficultly, here, k=0.7; T(t) is torque in drilling, Nm; n is rotational speed, rpm.

Equivalent correction coefficient is difficult to be determined, taken 0.7 here. According to the previous experiments, the torque, simplified to segmentation function, is shown in Figure 6. And rotational speed will be 108rpm.

The thermal loads of cutting edges are shown in Figure 7.

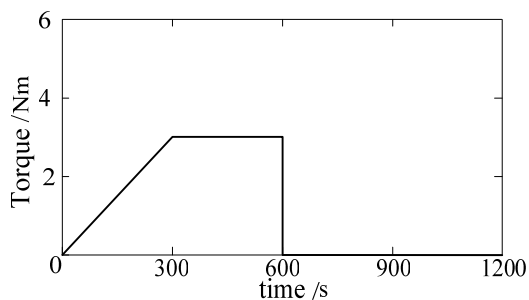


Figure 6. Torque versus Time in Simulation

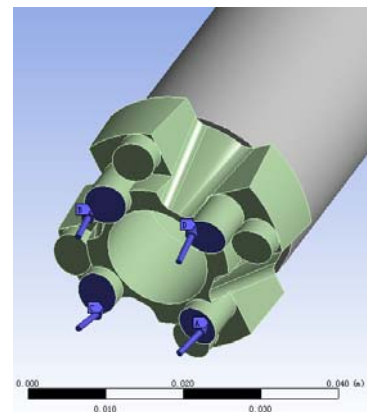


Figure 7. Thermal Loads of Cutting Edges

The material of bit and rod is C45 steel with smooth surface. The length of rod is 1000 mm with 500 mm in the vacuum tank for vacuum experiment. The simulation parameters are shown in Table 1.

Table 1. The Parameters of Simulation

Room temperature(°C)	density (kg/m ³)	thermal conductivity (W/m°C)		specific heat (J/kg°C)		emissivity	convection coefficient (W/m ² □)
20	7.85	0°C	52.34	20°C	461	0.24	5
		100°C	48.85	200°C	544		
		200°C	44.19				
		300°C	41.78				

The distribution of temperature field for the drill tool and the measuring point is shown in Figure 8. The result is show in Figure 9.

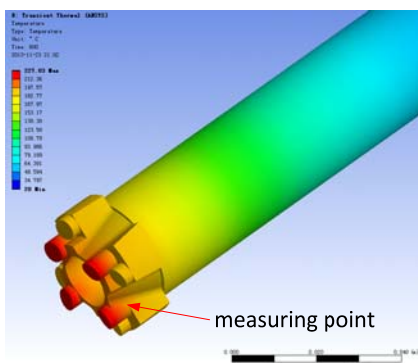


Figure 8. Distribution of Temperature Field for the Drill Tool and the Measuring Point

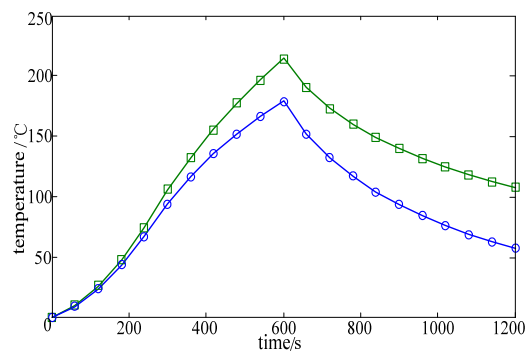


Figure 9. Temperatures of Measuring Point in Atmosphere and Vacuum versus Time in Simulation

It can be seen from Figure 9 that under the same Thermal load conditions, the temperature rise of measuring point in vacuum is higher than that in atmosphere, that conforms to the expectation. The difference of temperature is about 40°C.

4. Thermal Test in Vacuum and Atmosphere



a) drilling into Sandstone in vacuum



b) The sandstone after drilling

Figure 10. Pictures of Drilling Sandstone

The test process is shown in Figure 10 and Figure 11. In order to obtain the desired vacuum test environment, a rotary vane vacuum pump was used, which can achieve a

maximum vacuum of 1Pa. Comparing with the molecular pump, which could reach higher vacuum degree, rotary vane vacuum pump can withstand harsh dust environment. The existing vacuum pump requires 2-3 hours to obtain the necessary test environment. If a higher vacuum environment needed, the test time will increase exponentially. Considering above facts, a rotary vane vacuum pump was chosen to meet the minimum requirements for test environment.



a) drilling into loam brick in vacuum



b) The loam brick after drilling

Figure 11. Pictures of Drilling Loam Brick

The trial matrixs for test phase I and test phase II are as shown in Table 2 and Table 3, with their results.

Table 2. Thermal test trial matrix of phase I (room temperature 17°C)

No.	drilling subject	vacuum degree [Pa]	drilling parameters		drilling time[min]	feed maximum temperature[°C]	feed-stop maximum temperature[°C]
			rotational speed[rpm]	feed rate [mm/min]			
1001		170	108	2	feed 8.5/ feed-stop 1.5	200	230
1002	sandstone	normal atmosphere	108	2	feed 8.5/ feed-stop 1.5	100	114
1003		130	108	2	feed 8.5/ feed-stop 5	199	248
1004		normal atmosphere	108	2	feed 8.5/ feed-stop 5	104	138
1005		230	108	2	feed 12/ feed-stop 3	98	87
1006	loam brick	normal atmosphere	108	2	feed 12/ feed-stop 3	70	60
1007		200	108	4	feed 6/ feed-stop 3	168	224
1008		normal atmosphere	108	4	feed 6/ feed-stop 3	128	198

Table 3. Thermal Test Trial Matrix of Phase II (room temperature 20°C)

No.	drilling subject	vacuum degree [Pa]	drilling parameters		drilling time[min]	drilling depth[mm]	feed maximum temperature[°C]
			rotational speed[rpm]	feed rate [mm/min]			
2001		190	108	20	2.5	50	70
2002		87	108	2	25	50	263
2003	loam brick	150	54	2	6	12	35
2004		130	108	1	50	50	492
2005		100	54	1	50	50	96
2006		190	54	1	32	32	265
2007		84	108	1	35	35	378
2008	sandstone	40	108	2	25	50	407
2009		74	108	1	50	20	420
2010		35	108	2	25	50	414

Note: During test No. 2003, the rig breaks down, but the data is effective for analysis.

5. The Influence of the Vacuum on the Thermal Characteristics of the Drilling Process

The tests simulate the lunar surface vacuum conditions. According to the test plan matrix, two sets of test data, which are performed in uniform environmental conditions respectively, are chosen for comparison. The two are listed in Table 4 and Table 5. And the comparing curves are shown in Figure 12 and Figure 13.

Table 4. 1001-1002 Rigid Sandstone Experiment Data

No.	vacuum degree [Pa]	drilling parameters		drilling time[min]	feed maximum temperature[□]	feed-stop maximum temperature[□]
		rotational speed[rpm]	feed rate [mm/min]			
1001	170	108	2	feed 8.5/ feed-stop 1.5	200	230
1002	normal atmosphere	108	2	feed 8.5/ feed-stop 1.5	100	114

Table 5. 1005-1006 Rigid Clay Drilling Experiment Data

No.	vacuum degree [Pa]	drilling parameters		drilling time[min]	feed maximum temperature[□]	feed-stop maximum temperature[□]
		rotational speed[rpm]	feed rate [mm/min]			
1005	230	108	2	feed 12/ feed-stop 3	98	87
1006	normal atmosphere	108	2	feed 12/ feed-stop 3	70	60

It can be seen from Figure 6 and Figure 7 that under the same experimental conditions, the atmospheric test and the vacuum test have different results. Vacuum has a great influence on the drill bit temperature, and the temperature of bit under vacuum is almost double of that in atmosphere when the temperature reaches 200°C. The difference of the temperature in experiment higher than that in simulation.

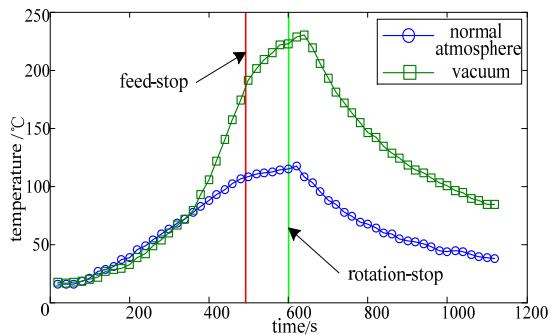


Figure 12. 1001 and 1002 Rigid Sandstone Drilling Temperature

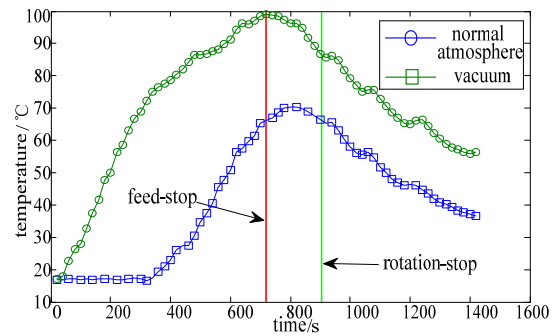


Figure 13. 1005 and 1006 Rigid Clay Drilling (2mm/min) Temperature Curve

6. Conclusion

The temperature and its influencing factors in drilling rigid regolith process is a great concern of space engineering, especially in vacuum. A preliminary experimental research on this issue is carried out in this paper. It can be seen from the experimental results that, in vacuum, the temperature of the drill will significantly rise. And the higher the temperature is, the deeper the effect shows. The experimental results show that the vacuum must be considered as one of the important factors during the study on the drill bit thermal characteristic.

The result in this paper is the first step of the study on lunar regolith drill thermal characteristics. The actual drilling process on Luna would be taken in a high vacuum environment, which is almost impossible to reach, and more accurate simulations will be carried out in further research.

Acknowledgements

This work was financially supported by the National Nature Science Foundation of China (Grant No. 51105092) and College Discipline Innovation Wisdom Plan of China (111 Project, Grant No. B07018).

References

- [1] Zhang H. From the Satellite to Lunar Probe. Shanghai: Shanghai Scientific and Technological Education Publishing. 2007.
- [2] Cui J, Hou X, Zhao D. Experimental Research on Temperature Rise of Bit in Drilling Normal and Low Temperature Lunar Soil Simulant. *Applied Mechanics and Materials*. 2013; 373: 2008-2014.
- [3] Cremers C, Birkebak R, Dawson J. *Thermal conductivity of fines from Apollo 11*. Proceedings of the Apollo 11 Lunar Science Conference. 1970; 3: 2045-2050.
- [4] Cremers C, Birkebak R. *Thermal conductivity of fines from Apollo 12*. Proceedings of the Second Lunar Science Conference. 1971; 3: 2311-2315.
- [5] Keihm S, Langseth M. *Surface brightness temperatures at the Apollo 17 heat flow site: Thermal conductivity of the upper 15cm regolith*. Proceedings of the Fourth Lunar Science Conference. 1980; 3: 2503-2513.